



## Long non-coding RNAs in *C. elegans*

Jin-Wu Nam and David Bartel

*Genome Res.* published online

Access the most recent version at doi:[10.1101/gr.140475.112](https://doi.org/10.1101/gr.140475.112)

---

<b>P&lt;P</b>	Published online in advance of the print journal.
<b>Accepted Preprint</b>	Peer-reviewed and accepted for publication but not copyedited or typeset; preprint is likely to differ from the final, published version.
<b>Open Access</b>	Freely available online through the <i>Genome Research</i> Open Access option.
<b>Creative Commons License</b>	This article is distributed exclusively by Cold Spring Harbor Laboratory Press for the first six months after the full-issue publication date (see <a href="http://genome.cshlp.org/site/misc/terms.xhtml">http://genome.cshlp.org/site/misc/terms.xhtml</a> ). After six months, it is available under a Creative Commons License (Attribution-NonCommercial 3.0 Unported License), as described at <a href="http://creativecommons.org/licenses/by-nc/3.0/">http://creativecommons.org/licenses/by-nc/3.0/</a> .
<b>Email alerting service</b>	Receive free email alerts when new articles cite this article - sign up in the box at the top right corner of the article or <a href="#">click here</a>

---

Advance online articles have been peer reviewed and accepted for publication but have not yet appeared in the paper journal (edited, typeset versions may be posted when available prior to final publication). Advance online articles are citable and establish publication priority; they are indexed by PubMed from initial publication. Citations to Advance online articles must include the digital object identifier (DOIs) and date of initial publication.

---

To subscribe to *Genome Research* go to:  
<http://genome.cshlp.org/subscriptions>

---

## Long non-coding RNAs in *C. elegans*

Jin-Wu Nam<sup>1,2,3</sup> and David P. Bartel<sup>1,2,3\*</sup>

<sup>1</sup>Whitehead Institute for Biomedical Research, Cambridge, MA 02142, USA

<sup>2</sup>Howard Hughes Medical Institute

<sup>3</sup>Department of Biology, Massachusetts Institute of Technology, Cambridge, MA 02139, USA

\*Correspondence: [dbartel@wi.mit.edu](mailto:dbartel@wi.mit.edu)

Running title: *C. elegans* lincRNAs

Keywords: long non-coding RNAs, gene annotation, gene expression, endogenous siRNAs

## ABSTRACT

Thousands of long non-coding RNAs (lncRNAs) have been found in vertebrate animals, a few of which have known biological roles. To better understand the genomics and features of lncRNAs in invertebrates, we used available RNA-seq, poly(A)-site, and ribosome-mapping data to identify lncRNAs of *C. elegans*. We found hundreds of long intervening ncRNAs (lincRNAs), which had single- or multi-exonic structures that did not overlap protein-coding transcripts, and about seventy antisense lncRNAs (ancRNAs), which were complementary to protein-coding transcripts. Compared to protein-coding genes, the lncRNA genes tended to be expressed in stage-dependent manner. Approximately 30% of the newly identified lincRNAs showed little signal for sequence conservation and mapped antisense to clusters of 22G or 26G endogenous siRNAs, as would be expected if they serve as templates and targets for these siRNAs. The other 70% tended to be more conserved and included lincRNAs with intriguing expression and sequence features associating them with processes such as dauer formation, male identity, sperm formation, and interaction with sperm-specific mRNAs. Our study provides a glimpse into the lncRNA content of a non-vertebrate animal and a resource for future studies of lncRNA function.

Data access: The data discussed in this publication have been deposited in NCBI's Gene Expression Omnibus and are accessible through GEO Series accession number GSE36394 (<http://www.ncbi.nlm.nih.gov/geo/query/acc.cgi?acc=GSE36394>).

## INTRODUCTION

Since the discovery of Xist, a lincRNA required for mammalian X-chromosome inactivation (Borsani et al. 1991; Brockdorff et al. 1992; Brown et al. 1992), thousands of other lincRNAs have been reported in mammals and other vertebrates (Okazaki et al. 2002; Numata et al. 2003; Carninci et al. 2005; Guttman et al. 2009; Gerstein et al. 2010; Guttman et al. 2010; Kim et al. 2010; Orom et al. 2010; Grabherr et al. 2011; Pauli et al. 2011b; Ulitsky et al. 2011; Wang et al. 2011b). When considering their genomic origins relative to annotated protein-coding genes, most lincRNAs are classified either as long intervening ncRNAs (lincRNAs), which derive from loci that do not overlap the exons of protein-coding genes, or as antisense ncRNAs (ancRNAs), which derive from the opposite strand of the protein-coding gene such that they have potential to pair to the mature mRNA. lincRNAs are also called long intergenic RNAs, and ancRNAs are also called natural antisense transcripts (NATs). Most lincRNA gene models resemble those of protein-coding genes in terms of the CpG islands, multi-exonic structures, and poly(A)-signals, but they have no more than chance potential to code for protein and are translated poorly from relatively short reading frames, if at all (Numata et al. 2003; Guttman et al. 2010; Ingolia et al. 2011).

Although for most lincRNAs functions have not yet been investigated, some are known to play gene-regulatory roles or other biological roles in cells or during embryonic development (Goodrich and Kugel 2006; Mercer et al. 2009; Huarte and Rinn 2010; Koziol and Rinn 2011; Pauli et al. 2011a; Tsai et al. 2011). For example, HOTAIR is a 2.2-kb lincRNA that recruits the polycomb complex to modify the chromatin state of *HOX* genes to repress their transcription (Rinn et al. 2007; Gupta et al. 2010; Tsai et al. 2010), and lincRNA-*p21* is induced by TP53 upon DNA damage or oncogenic stress and causes the widespread suppression of numerous genes by recruiting the repressor protein hnRNP-K, thereby acting as a potential tumor suppressor (Huarte et al. 2010). Additional lincRNAs are also associated with transcriptional regulation (Martianov et al. 2007; Wang et al. 2008; Zhao et al. 2008), whereas Malat1 can regulate genes at the posttranscriptional level by titrating an SR protein that regulates alternative

mRNA splicing (Ji et al. 2003; Tripathi et al. 2010). Other examples include the megamind and cyrano lincRNAs, which are conserved from human to fish and play important roles in embryonic development (Ulitsky et al. 2011).

Compared to most mRNAs, lincRNAs generally accumulate to lower levels, and although some have detectable sequence conservation, many have no more conservation than expected by chance, implying that a large subset of lincRNAs are either biochemical noise or play newly evolved, species-specific roles (Carninci et al. 2005; Guttman et al. 2010; Cabili et al. 2011; Ulitsky et al. 2011). However, some lincRNAs without detectable sequence conservation derive from syntenic loci and have conserved gene structure (conserved exon size and number), suggesting that the apparent lack of conservation might reflect technical difficulties, such as greater challenges in accurate sequence alignment (Ulitsky et al. 2011).

lincRNAs are also found in invertebrates, as illustrated by the *roX1* and *roX2* lincRNAs, which are required for dosage compensation in flies (Larschan et al. 2011). In *C. elegans*, a subgroup of the modENCODE consortium carried out RNA-seq on poly(A)-selected RNA, which enabled annotation of 64,824 transcripts from 21,733 genes that would be expected to include some with little coding potential (Hillier et al. 2009; Gerstein et al. 2010). In parallel, using orthologous criteria (tiling array data, predicted RNA secondary structures, and sequence conservation) another subgroup of the consortium predicted ~7,000 ncRNA candidates, 1,678 of which did not overlap with annotated protein-coding genes (Gerstein et al. 2010; Lu et al. 2010). However, we noticed that the overlap between these 1,678 ncRNA candidates and the 64,824 transcripts identified by RNA-seq included only 24 transcripts, which is smaller than the chance expectation of  $120 \pm 8$  (mean  $\pm$  sd for 10 cohorts of length-matched loci falling between protein-coding genes), implying that the confident identification of lincRNAs in *C. elegans* might benefit from additional analyses.

One potential function of non-coding transcripts is to serve as precursors or templates for the production of endogenous guide RNAs for RNAi or related silencing pathways. For example, the *BIC* proto-oncogene ncRNA was later reannotated as the primary transcript of the mammalian miR-155 miRNA (Lagos-Quintana et al. 2002). *C. elegans* has Piwi-interacting RNAs (21U-RNAs) and many endogenous small interfering RNAs (endo-siRNAs), including 22G-RNAs and 26G-RNAs (which tend to start with a G and be 22 and 26 nt long, respectively) (Ruby et al. 2006; Batista et al. 2008). The most abundant class of endo-siRNAs, 22G-RNAs, are produced by RRF-1 and EGO-1, RNA-dependent RNA polymerases (RDRPs) acting on template transcripts, and then become associated with worm-specific argonautes (WAGO proteins and CSR-1) (Ruby et al. 2006; Claycomb et al. 2009; Gu et al. 2009). CSR-1-associated 22G-RNAs target thousands of germline-specific genes, tend to map to the exons of those mRNAs and are implicated in chromosome segregation (Claycomb et al. 2009). By contrast, WAGO-1-associated 22G-RNAs often map to both introns and exons of pre-mRNAs and have unknown biological roles (Gu et al. 2009). In addition, some 22G-RNAs map to clusters of loci lacking annotated transcripts. Because they did not correspond to known transcripts, such RNAs were initially annotated as a unique class of small-RNAs (tiny non-coding RNAs, or tncRNAs), distinct from endogenous siRNAs (Ambros et al. 2003). However, as high-throughput sequencing revealed their similarities to endo-siRNAs, tncRNAs were reclassified as siRNAs, with the presumption that they derive from ncRNA template transcripts that still needed to be identified (Ruby et al. 2006; Pak and Fire 2007).

In this study, we identify lncRNA genes, starting with a pipeline that constructs transcript annotations *de novo* by combining data from RNA-seq and poly(A)-site mapping, and then removes those with detectable protein-coding potential or experimentally observed ribosome association. Hundreds of lncRNAs that have either single- or multi-exonic transcript structures with poly(A) signals were found, thereby providing a glimpse into the lncRNA content of a non-vertebrate animal.

## RESULTS

### ***De novo* gene annotation using multimodal transcriptome data**

We first developed a pipeline for global *de novo* annotation of transcripts from RNA-seq and poly(A)-site datasets. Because our focus was on lncRNAs, we chose not to consider information helpful for predicting protein-coding transcripts (such as, sequence conservation, homology to known genes, codon usage or coding potential) reasoning that by avoiding the consideration of this information we could use our accuracy for identifying previously annotated mRNAs to indicate accuracy for identifying lncRNAs.

Using the TopHat, an alignment program that maps RNA-seq reads to putative exon junctions as well as genomic sequence (Trapnell et al. 2009), we mapped more than 1 billion reads (including 50 million exon-junction reads) from 25 non-strand-specific RNA-seq datasets (Gerstein et al. 2010; Lamm et al. 2011) and more than 80 million reads (including 5 million exon-junction reads) from 10 strand-specific RNA-seq datasets (Lamm et al. 2011) (Figure 1A, Tables S1A and B). To avoid false-positive exon-junction hits, we required that the inferred introns be  $\geq 40$  nt and  $\leq 3058$  nt, which would capture all but the shortest and longest 1% of introns within annotated protein-coding genes. Using the Cufflinks program (Trapnell et al. 2010), *de novo* gene annotations were constructed for non-strand-specific and strand-specific RNA-seq datasets, respectively (Figure 1A). As expected, the annotations based on larger amounts of data (non-strand-specific RNA-seq) were more sensitive, whereas the annotations based on more informative reads (strand-specific RNA-seq) were more specific (Table S1C), especially in instances of convergent overlapping transcripts, which are quite common in *C. elegans*, where they include a sixth of the mRNAs (Jan et al. 2011).

To maximize both sensitivity and specificity, we designed scripts that 1) used information from the strand-specific reads to correct the non-strand-specific annotations, systematically evaluating each exon for strand-specific support and for transitions in the strand supported (Figure S1A), 2) incorporated

information from exon-junction hits that was not incorporated in the original annotations from either the strand-specific or non-strand-specific data (Figure S1B), 3) used poly(A) sites identified using 3P-seq [poly(A) position profiling by sequencing (Jan et al. 2011)], to assign 3' ends of most transcripts (Figure S1B). The resulting 82,462 transcripts from 24,644 loci included 84.1% of the nucleotides falling within the RefSeq protein-coding transcripts (ce6), and the RefSeq protein-coding transcripts made up 66.3% of the nucleotides within the 82,462 transcripts (Table S1C). These percentages did not perfectly reflect annotation sensitivity and specificity, in part because these RefSeq protein-coding transcripts were missing any lncRNAs that might be present in *C. elegans* as well as the 3' UTRs of many protein-coding transcripts (Mangone et al. 2010; Jan et al. 2011). Moreover, based on observations in vertebrates, where lncRNAs tend to be expressed at levels lower than those of protein-coding transcripts (Guttman et al. 2010; Cabili et al. ; Ulitsky et al. 2011), the sensitivity for lncRNAs was expected to be lower than that of protein-coding transcripts (Figure S2). Nonetheless, the improvement of these percentages over those of our initial *de novo* annotations suggested even greater sensitivity than that achieved for the annotations from non-strand-specific data and even greater specificity than that achieved for the annotations from strand-specific data (Table S1C).

The 82,462 transcript isoforms (including 3' UTR isoforms) consisted of 78,940 multi-exon transcripts and 3,521 single-exon transcripts, which together derived from 24,644 unique loci (Figure 1A). Most of the loci overlapped with those annotated by modENCODE (Figure 1B), as expected because both sets of annotations were based largely on the same non-strand-specific RNA-seq and 3P-seq datasets (Gerstein et al. 2010). Nonetheless, our annotations included 3,745 unique loci. In addition, 1,347 modENCODE loci were undetected, presumably because we did not include EST data or the additional types of information useful for predicting protein-coding loci.

### **Genome-wide identification of lncRNAs**



To identify lincRNAs, our 24,644 loci were filtered to remove those that overlapped the sense strand of annotated protein-coding genes, pseudogenes, ribosomal RNA, tRNA, miRNA, and other known classes of ncRNAs (Ce6 and Ensembl version 57). Of the 3,291 loci (5,029 transcript isoforms) that remained after this filtering, 1,546 (2,522 transcript isoforms) with  $\geq 100$  nt of antisense overlap with pre-mRNAs or other annotated transcripts were classified as ancRNA candidates, and the remaining 1,745 loci (2,507 transcript isoforms) were designated lincRNA candidates (Figure 1A).

For each of these lincRNA candidates, coding potential was evaluated, removing those with 1) scores  $\geq -1.0$  when using the coding potential calculation (CPC) program (Jia et al. 2010) (Figure S3A), 2) marginal confidence in coding potential ( $P \leq 0.01$ ) as evaluated using the RNAcode program (Washietl et al. 2011), or 3) evidence of ribosome association in an experiment that sequenced transcripts sedimenting with polyribosomes (polyribosome reads/RNA-seq RPKM  $\geq 0.1$ ) (Lamm et al. 2011) (Figure S3B). This filtering retained 882 potential lincRNA loci (Figure 1C) and 352 potential ancRNA loci (Figure 1D). Further analysis using the 3P-seq data to identify transcripts with evidence of a poly(A) tail recovered 251 lincRNA loci, which were represented by 427 alternative splicing/3'-end isoforms, and 66 ancRNA loci, which were represented by 114 alternative splicing/3'-end isoforms (Figure 1E and Tables S2). The lincRNA loci were named using *linc* gene classifier (i.e., *linc-1* through *linc-251*), and the ancRNA loci were named using *anr* classifier (an acronym for ancRNA that is also the reverse of "RNA"). The search for lincRNA poly(A) sites included more genomic regions than did the previous analysis of UTRs (Jan et al. 2011) and therefore identified poly(A) sites that had not been previously recognized (Figure S4). The mean lengths of the lincRNAs and ancRNAs with assigned poly(A) sites were 774 and 776 nt, respectively, which were shorter than the mean length of mRNAs ( $\sim 2.2$  kb) (Tables S2A and S2B).

The potential lincRNAs with assigned poly(A) sites (Tables S2C and S2D) were carried forward as our set of *C. elegans* lincRNAs because they were the ones most confidently annotated as independent

transcripts. Of the 251 lincRNA loci, 157 overlapped a modENCODE gene model (Gerstein et al. 2010), and 9 overlapped one of the 1,678 ncRNA candidates (Lu et al. 2010). Of the 66 ancRNA loci, 32 overlapped a modENCODE gene model (Gerstein et al. 2010). Although identified with less confidence, the potential lincRNAs without 3P-seq support (Tables S2E and S2F) are likely to include some interesting transcripts, including canonical lincRNAs that have poly(A) tails but lacked 3P-seq support because they are not highly expressed at the stages with 3P-seq data. Other potentially interesting transcripts, presumably including some enhancer-associated transcripts, might not be poly-adenylated. One highly conserved non-coding RNA excluded because it lacked a poly(A) tail was the metazoa signal-recognition particle RNA (Table S2E).

### **mRNA partners of ancRNAs**

Of the 66 ancRNAs, 42 were fully embedded within pre-mRNA partners (16 fully within introns), 13 had divergent overlap with their pre-mRNA partner, six had convergent overlap, and five fully encompassed their pre-mRNA or ncRNA partner. About half of the mRNA partners were hypothetical genes without confirmed expression, which raised the possibility that many might not be authentic mRNAs. For mRNA partners in each subgroup, we found no evidence for common functions (as measured using Gene Ontology enrichment). Expression analysis for each subgroup revealed that only convergent pairs tended to be anti-correlated each other, and that for convergent pairs more examples will be needed to confirm statistical significance (Figure S5; mean  $r = -0.19$ ,  $P = 0.047$ , one-sample t-test).

### **Occasional trans-splicing of lincRNAs**

Identifying transcript start sites (TSSs) is challenging in *C. elegans* because trans-splicing often replaces the 5' end of pre-mRNAs with a splice-leader sequence (Figure 1F). Approximately 70% of mRNAs possess splice leaders at their 5' end, most of which have unknown TSSs. To examine whether lincRNAs also possess splice leaders we looked for evidence of chimeric RNA-seq reads that did not map to

genome and instead had at least 12 nt of splice leader sequence (choosing from the ten leaders most frequently observed for mRNA) fused to sequences in the 5' regions of lincRNAs and mRNAs (Figure 1F). Of the 343,660 RNA-seq reads that contained the 3' part of a splice leader but did not match the genome, 87,194 were chimeric reads that resulted from trans-splicing near the 5' end (within -500 to 100 nt) of mRNAs for 20,587 unique RefSeq genes. This analysis captured 6,624 unique junctions with at least two reads (Table S3A). In contrast, only 65 chimeric reads capturing only 16 unique junctions with at least two reads (Table S3B) represented trans-splicing to the 251 lincRNAs (within -500 to 100 nt of the 5' end inferred by RNA-seq reads). Even when comparing to expression-matched mRNAs, the number of chimeric reads and unique trans-splicing junctions were more abundant for mRNAs than for lincRNAs (Figure 1G).

Trans-splicing frequently serves to separate polycistronic pre-mRNAs into individual mRNAs. In *C. elegans*, >1000 operons have been identified, each containing two to eight genes, and accounting for 15% of all *C. elegans* genes (Spieth et al. 1993; Blumenthal and Gleason 2003). Among the 251 lincRNA genes, 10 tandem clusters were found (Table S4), each containing lincRNA genes within 1kb of each other. For example, *linc-58* is next to *linc-23*, with only 320 bp separating the two genes (Figure S6). The fraction of clustered lincRNA genes (4.0%) was much less than that of protein-coding genes, and none of corresponding lincRNAs were associated with the SL2 sequence, which is used for polycistronic pre-mRNAs (Spieth et al. 1993). These observations suggest that lincRNA genes are less likely than protein-coding genes to have the operon-like transcript structure. Because trans-splicing tends to occur very close to the start codon, the splice leader is also thought to confer more efficient translation initiation (Blumenthal and Steward 1997; Lall et al. 2004). This role for the splice leader would help explain why trans-splicing is more frequent for mRNAs than for lincRNAs. Indeed, we found that for mRNAs, the AUG translational start codon was the codon most enriched in the 30 nt downstream of the junctions (adjusted  $P = 8 \times 10^{-5}$ ), whereas for lincRNAs, other codons were enriched instead (GAC, adjusted  $P = 5.5$

$\times 10^{-4}$  and GCC, adjusted  $P = 8.6 \times 10^{-4}$ , Table S3C). Taken together, our results show that some *C. elegans* lincRNA primary transcripts are trans-spliced, but for the few that are trans-spliced, the trans-splicing plays a role apart from separating polycistronic transcripts or enhancing translation initiation.

### **lincRNAs antisense to endo-siRNA clusters**

When mapping published (Batista et al. 2008; Gu et al. 2009) and newly generated small-RNA sequencing data (Table S5), we noticed that highly expressed endo-siRNAs often mapped antisense to lincRNAs (Examples in Figure S7). Of the 251 lincRNAs, 65 were antisense to either 22G-RNAs (small-RNA RPKM  $\geq 5$ ) or 26G-RNAs (small-RNA RPKM  $\geq 5$ ) in at least one developmental stage (Table S6 and Figure S8A). This fraction of lincRNAs (25.9%) was comparable to that of protein-coding genes antisense to endo-siRNAs (32.1%). As observed for mRNAs, more highly expressed lincRNAs tended to map antisense to endo-siRNAs (Table S6 and Figures 2A and S8A). For example, 33% of 112 lincRNAs with mean RPKM  $\geq 1$  mapped antisense to 22G-RNAs (small-RNA RPKM  $\geq 5$ ) in L4 or adult stages (Figure 2A), whereas only 11.5% of lincRNAs with mean RPKM  $< 1$  mapped antisense to 22G-RNAs in the same stages (Figure S8A and Table 1).

Although overall lincRNAs resembled mRNAs in mapping antisense to endo-siRNAs, lincRNAs tended to map to some sub-classes of endo-siRNAs more than to others. About 35% of both lincRNAs and mRNAs with RPKM  $\geq 1$  in adult mapped antisense to CSR-1–associated 22G-RNAs ( $P = 0.73$ , Fisher's exact test), whereas the fraction antisense to WAGO-1–associated 22G-RNAs was much higher for lincRNAs than for mRNAs (23.5% and 10.6%, respectively,  $P < 0.0018$ , Fisher's exact test; Table 1). Moreover, 25% of 112 lincRNAs with mean RPKM  $\geq 1$  mapped antisense to 26G-RNAs (small-RNA RPKM  $\geq 5$ ) in either embryo or L4 stages—a fraction  $>6$  times higher than that of mRNAs ( $P < 10^{-14}$ ), which increases to 100 times higher when considering 26G-RNAs in the embryo stage ( $P < 10^{-25}$ ; Table 1).

Many of the endo-siRNAs that mapped to previously unannotated regions of the genome mapped antisense to our newly annotated lincRNAs. After grouping the 22G-RNAs mapping within 100 nt of each other into clusters and ranking the clusters by the number of 22G-RNA reads, we found that the first and seventh clusters mapped antisense to *linc-25* and *linc-38*, respectively (Figure 2B, Figure S7A). Three other clusters mapped antisense to pseudogenes, another class of ncRNA gene (Figure 2B). A similar analysis of 26G-RNA clusters (grouping those mapping within 1000 nt of each other) found that six of the top 30 clusters mapped antisense to lincRNAs and that one mapped antisense to a pseudogene (Figure 2C and Figure S7B). Moreover, three 22G-RNA and three 26G-RNA clusters mapped antisense to newly annotated transcripts that did not pass our cutoffs for lincRNA annotation because they satisfied only two of the three filtering criteria (Figures 1C and 2B–C). Overall, the lincRNA annotations and other recent gene-annotation improvements (Gerstein et al. 2010) provided substantial insight into the origins of endo-siRNAs, with most of the siRNA clusters that previously mapped to unannotated regions now mapping antisense to newly annotated transcripts (Figures S8B and C). Of those clusters mapping predominantly (90% of reads) to one annotation, between 4–19% (depending on the stage) mapped antisense to lincRNAs, an 8–65-fold enrichment compared to mRNAs (Figures S8B and C;  $P < 0.0025$  to  $< 10^{-16}$ ).

In RNAi-treated *C. elegans*, target mRNAs are down-regulated at both the post-transcriptional and transcriptional levels (Montgomery et al. 1998). RNAi-mediated transcriptional repression occurs co-transcriptionally, whereby nuclear-localized siRNAs inhibit RNA Polymerase II elongation and facilitate the establishment of histone H3 lysine 9 methylation (H3K9me3) (Guang et al. 2010; Burkhart et al. 2011; Gu et al. 2012). By analogy, the lincRNAs antisense to endo-siRNAs presumably template the production of the corresponding siRNAs, some of which recruit heterochromatin factors to silence regions from which they originate. Supporting this conjecture, genes for lincRNAs antisense to 22G-RNAs and 26G-RNAs tended to map to the ends of chromosomes, which have a higher density of the H3K9me3

heterochromatic mark (Figure S9A), and these genes had significantly more H3K9me3 signal compared to genes for other lincRNAs (Figures S9B). Moreover, the H3K9me3 signal at these lincRNAs depended on the *nrde-2* nuclear RNAi pathway (Figure S9C).

### Sequence composition and conservation of nematode lincRNAs

The A/U contents of both lincRNA and ancRNA sequences were comparable to that of sampled intergenic regions, falling between that of CDS/5' UTRs and that of 3' UTRs (Figure 3A), as observed for zebrafish and mammalian lincRNAs (Ulitsky et al. 2011). No base-composition differences were observed between lincRNAs antisense to endo-siRNAs and other lincRNAs (Figure 3B).

The extent of sequence similarity (E-value  $\leq 10^{-10}$ ) between lincRNAs (34 out of 251, 13.5%) was much higher than that between mRNAs ( $1.2 \pm 1.1\%$  for 10 random cohorts of 251 mRNAs,  $P < 10^{-10}$ , Fisher's exact test; Figure S10), due in part to the increased presence of repeat elements in lincRNA sequences (47% of lincRNAs with a similar sequence among them harbored an annotated repeat element). The fraction of lincRNAs with repeat sequences (34, 13.5%) was much greater than for mRNAs (2.5%,  $P < 10^{-14}$ , Fisher's exact test; Figures 3C and D). Repeat elements that lincRNAs shared included helitron, satellite sequences, LINE elements, and transposable repeat elements.

To examine the overall conservation of nematode lincRNAs, we used the phastCons scores (Siepel et al. 2005), focusing on residues that were aligned in the whole-genome sequence alignments but did not map to annotated repeats. The fraction of lincRNA residues aligned in the whole-genome alignments was about 27%, which was much smaller than those of mRNA CDS (88%) and 3' UTRs (55%) and comparable to those of mRNA introns (25%) and intergenic controls, termed control exons (27%; Figure 3E). We compared the conservation of exons and introns of lincRNA to those of length-matched exons and introns of protein-coding genes. The aligned lincRNA exons were more conserved than corresponding lincRNA introns but much less conserved than CDS exons and 3' UTRs, and about as

conserved as mRNA introns and length-matched control exons (Figure 3F). The conservation of lincRNAs was anti-correlated with the density of corresponding endo-siRNAs (Figure 3G), such that lincRNAs without antisense 22G-RNAs (64.9% of 251 lincRNAs) were more conserved than both mRNA introns and control exons (Figures 3F and G). These results suggest the existence of at least two different subclasses of lincRNAs: nonconserved ones associated with endo-siRNAs and moderately conserved ones not associated with endo-siRNAs. Likewise, some protein-coding genes and pseudogenes to which certain classes of endo-siRNAs map appear particularly non-conserved (Fischer et al. 2011). The lower conservation of lincRNAs associated with endo-siRNAs is consistent with origins from heterochromatic regions, which are often poorly conserved.

Some vertebrate lincRNAs contain short conserved regions, which play important roles despite rapid sequence evolution elsewhere in the lincRNAs (Ulitsky et al. 2011). We examined whole-genome sequence alignments (Siepel et al. 2005) to check whether nematode lincRNAs also have short evolutionally conserved sequence elements. Of lincRNA exons that had any conserved element, only ~30% had a conserved segment > 50 nt (phastCons score  $\geq 0.5$ ), whereas, of CDS exons that had any conserved element, ~60% had a conserved segment > 50 nt ( $P < 3 \times 10^{-8}$ , KS-test; Figure 3H and S11). Thus, as in vertebrates, the conserved lincRNAs tend to have shorter regions of conservation than do conserved mRNAs.

### **Developmental expression of nematode lincRNAs**

In vertebrates, lincRNAs tend to be expressed in a development-specific manner (Cabili et al. 2011; Ulitsky et al. 2011). To examine if this was also the case for *C. elegans* lincRNAs, we compared for each gene model the maximum expression among 10 developmental stages to the mean expression over the remaining 9 stages (Figure 4A and Table S7A). By this metric, lincRNAs tended to be expressed more differentially than did mRNAs, with median fold difference between maximum and mean RPKMs of 5.5

for lincRNAs, compared to 3.7 for mRNAs ( $P < 10^{-10}$ , KS-test; Figure 4A). The most extreme example was linc-3, which had an RPKM of 1002 in dauer stage, which was ten thousand times greater than the average of the 9 other stages and conditions (Figures 4A and B). Of the 114 unique lincRNAs with maximum RPKM  $\geq 8$ , 33 had ratios exceeding 10, and linc-1 had the highest maximum RPKM, which exceeded 1360 in male-related stages (Tables S7A and B). The more specific expression of many lincRNAs might partly explain their lower overall expression levels.

To study co-expression of lincRNAs in specific conditions or developmental stages, we performed a CLICK clustering analysis (Sharan et al. 2003), based on Pearson correlation of z cores derived from expression distributions for each lincRNA. Four major co-expressed clusters were found, accounting for 27 embryo-specific, 53 early larval-specific, 55 sperm-specific, and 30 dauer-specific lincRNAs (Figure 4C and Tables S7C–F). Using a similar approach, we also found two co-expressed clusters comprising 19 sperm-specific and 28 L3-specific ancRNAs (Figure S12 and Tables S7G–I). As expected if some lincRNAs were templates of siRNAs, the sperm-specific lincRNAs were more frequently antisense to endo-siRNAs. Although two embryo-specific lincRNAs, four sperm-specific lincRNAs and two early-larval-specific lincRNAs were transcribed from genes within 10 kb of each other, most lincRNAs in each expression cluster were from genes that were not close together (Tables S7C–F).

The expression relationships between two neighboring genes can correlate with their orientations with respect to each other, with tandem or divergent genes showing a greater tendency to be co-expressed (Korbel et al. 2004; Chen and Stein 2006; Kensche et al. 2008; Chen et al. 2010; Wang et al. 2011a). We examined the extent to which lincRNA genes were co-expressed with their closest neighboring protein-coding gene (limiting the analysis to genes within 1 kb of each other, which excluded 104 of the 251 lincRNAs; Figure S13). Expression of the lincRNA and nearest protein-coding gene tended to be correlated, especially for the gene pairs in tandem and divergent orientations (Figure 4D). Longer-range



correlations were also observed for large clusters of genes within 200 kb regions (Table S8). For instance, within a 200 kb region centered on the dauer-specific *linc-3* gene, for which expression peaked in the dauer-entry stage (Figures 5A and B), the protein-coding genes also tended to be expressed in a dauer-specific manner, peaking after dauer entry (Figure 5C). As a result, the expression correlations between *linc-3* and each of the 59 genes in this larger region tended to be higher than that for 1000 cohorts of number-matched controls (mean  $r = 0.23$ , adjusted  $P < 4 \times 10^{-7}$ , one-sample t-test). This region included genes for serpentine receptors, which are seven trans-membrane G-couple chemo-receptors thought to function in dauer pheromone signaling pathway (Kim et al. 2009; McGrath et al. 2011). The functions of these co-expressed neighboring genes supported the idea that *linc-3* might also play a role in dauer formation or maintenance. Although short- and longer-range correlations were observed between the expression of lincRNAs genes and neighboring protein-coding genes, the correlations did not significantly differ from those observed between two neighboring protein-coding genes (Figure 4D). These results resembled those observed in vertebrates (Ulitsky et al. 2011) and suggested that compared to protein-coding genes, the lincRNA genes were no more likely to be misannotated extensions of neighboring genes and no more likely to influence expression of their neighboring genes.

### **Expression correlation of a lincRNA and complementary mRNAs**

Ten lincRNAs had a long region significantly similar to the sense strand of an mRNA ( $\geq 100$  nt, E-value  $< 10^{-51}$ ; Table S9A) and six lincRNAs had a long region significantly antisense to an mRNA ( $\geq 100$  nt, E-value  $< 10^{-51}$ ; Table S9B). Although these 12 unique lincRNAs might either derive from pseudogenes of protein-coding genes or simply share a common repeat element (Tables S9A and B), they nonetheless represented only 4.5% of our annotated lincRNAs, a much lower fraction than observed for mRNAs with homology to other mRNAs (19%).

Examination of shorter regions of homology identified 46 lincRNAs aligning antisense to one or more mRNAs (E-value  $<10^{-5}$ ), comprising 197 gene pairs (Table S10A). This fraction (18.3%) was significantly higher than that observed for number- and length-matched mRNA sequences ( $10.4 \pm 1.6\%$ , comprising an average of 42 pairs for 100 cohorts of computational controls,  $P < 0.0076$ , Fisher's exact test).

However, when excluding lincRNAs (and mRNA controls) associated with repeat elements, only 30 aligned antisense to one or more mRNAs, and the fraction of lincRNAs with antisense matches (13.8%) was not significantly higher than that for the controls (11.5%,  $P = 0.28$ ). These results indicated that the tendency to map antisense to short region of mRNAs occurred through repeat elements, raising the question as to whether it occurred by chance or has functional implications. Even after controlling for repeats, the number of the antisense pairs (104) was twice as high for the lincRNAs than for mRNA controls ( $40 \pm 17$ ), largely because a short conserved region of *linc-85* mapped antisense to 37 members of a large gene family encoding major sperm proteins and their hypothetical paralogs (Figure 6). These 37–52 nt regions of complementarity did not trigger endo-siRNAs. Overall there was not a strong tendency for the expression of *linc-85* or that of other lincRNAs with short regions of antisense complementarity to be anti-correlated with expression of their complementary mRNAs (Table S10B).

## DISCUSSION

Methods for annotating lncRNAs are improving but are still far from perfect. As with lists from previous efforts in other species, our lists of *C. elegans* ancRNAs and lincRNAs contain some very confident annotations and others that are less confident, primarily because they are not as well supported in the RNA-seq and 3P-seq datasets. The lower expression of lincRNAs compared to mRNAs has been used as evidence that they represent transcriptional noise or lack biological significance (Birney et al. 2007; Clark et al. 2011). However, the lower expression level might be due in part to their tissue, stage, and condition-specific expression patterns. Although we identified hundreds of lncRNAs in *C. elegans*, we suspect that with additional data more lncRNAs will be confidently and accurately annotated in this species. These will include many genes that lacked exon-junction reads for one of their introns and thus were missed because the unannotated intron disrupted connectivity to a 3P-supported poly(A) site. In fact, even after considering lincRNAs and the available RNA-seq data, some clusters of endo-siRNAs and 8436 poly(A) sites (13.2%) identified using 3P-seq remain unassociated with known gene models. Other lncRNAs that remain unannotated include those with tandom overlap with protein-coding genes, as we excluded any candidates with even a single nucleotide of sense overlap because of the difficulties in distinguishing between authentic lincRNAs and alternative 5' or 3' extensions of known genes.

Other potential sources of false-negatives in our lncRNA datasets were the stringent criteria used to filter out potential protein-coding genes. Most notable was our use of RNAcode (Washietl et al. 2011), an algorithm that compares the rates of synonymous and non-synonymous changes in whole-genome alignments to find evidence of conserved protein-coding potential. Because RNAcode can evaluate only sequences that are aligned to other genomes, any lncRNAs genes mistakenly flagged and removed by the algorithm would be conserved in other species and thus would be among those most attractive for experimental follow-up. When applying less stringent criteria (CPC < 0 and no consideration of RNAcode

and polyribosome association), an additional 133 lincRNA and 102 ancRNA candidates were identified (Table S11).

Another source of false negatives might have been our exclusion of annotated protein-coding genes, particularly the hypothetical protein-coding genes. With this in mind, we tested the coding potential of 19,907 annotated protein-coding genes. Eleven passed our criteria for annotation as potential lincRNAs and three of these also had 3P-seq-supported poly(A) sites (Table S12). Nine had been classified as hypothetical proteins and the other two were fungus- and bacteria-response genes. None had evidence for trans-splicing.

Although more lincRNAs will undoubtedly be found, the identification of lincRNAs and ancRNAs in *C. elegans*, with initial characterization of their evolution, genomics, and expression, provides a starting point for the study of lincRNA biology in an invertebrate animal. For some of the lincRNAs, expression or sequence features already associate them with processes such as dauer formation, male identity, sperm formation, and interaction with sperm-specific mRNAs. The study of these and other newly identified lincRNAs in *C. elegans*, with its established tools for rapid molecular genetic analyses, can now contribute to the understanding of the fascinating biology and mechanisms of these enigmatic transcripts.

## METHODS

### Data sources

*C. elegans* genome assembly WS190/ce6 was used throughout the study. For comparison to our *de novo* gene annotations and to analyze endo-siRNA clusters, NCBI RefSeq gene annotations (ce6, version Oct-3-2010) were used. To filter *de novo* transcripts overlapping with annotated genes, NCBI RefSeq gene annotation (ce6, version Oct-3-2010) and Ensembl annotations (version 57) were used. To find repeat loci, we used UCSC repeat-masking data (Jurka 2000). All public RNA-seq data and polyribosome data were obtained from NCBI SRA (SRA003622) and NCBI GEO (GSE22410 and GSE19414). 3P-seq data were taken from NCBI GEO (GSE24924). Small-RNA data were from previous studies, supplemented with newly acquired 5'-monophosphate-independent sequencing of small RNAs from L4 and adult stages (Table S5). Small-RNA sequencing was as described (Batista et al. 2008).

### Analysis of start codon enrichment.

The frequencies of the AUG start codon in the 30 nt downstream of trans-splicing sites of lincRNAs and mRNAs were compared to the background frequency observed within –500 to 100 nt of the trans-splicing sites. The *P* values were estimated by the hypergeometric test and adjusted by the Bonferroni correction.

### Expression correlation analysis

To measure expression correlation between mRNAs and lincRNAs, and among lincRNAs, we used RPKM values across 35 different developmental stages/conditions. To measure expression correlation among ancRNAs, we used RPKM values across 10 different stages that have strand-specific RNA-seq data.

### Sequence conservation analysis

For the comparisons, we excluded intronic regions and 3' UTRs with sense overlap with an RNAcode region ( $P \leq 0.01$ ) because lincRNAs did not include those regions, and then randomly sampled 1000

exons and introns, and 500 3' UTRs from genes. The introns were limited to those that did not overlap with any exons of alternative isoforms. For control exons, we considered intergenic regions, again excluding any region with sense overlap with an RNAcode region, and then randomly sampled 500 exon-length-matched regions. For each region, we calculated the mean phastCons score (Siepel et al. 2005), which was then adjusted by the fraction of residues aligned in multiple-genome alignments.

### **Additional bioinformatic analysis**

To find sequence-similar lincRNAs and mRNAs and to find antisense-matching mRNAs, NCBI BLASTN was used with the parameter “blastn -e 0.001 -K 1” and E-value cutoff of  $10^{-10}$  for lincRNA,  $10^{-51}$  for mRNAs, and  $10^{-5}$  for antisense-matching mRNAs.

### **DATA ACCESS**

The data discussed in this publication have been deposited in NCBI's Gene Expression Omnibus (Edgar et al. 2002) and are accessible through GEO Series accession number GSE36394 (<http://www.ncbi.nlm.nih.gov/geo/query/acc.cgi?acc=GSE36394>).

### **ACKNOWLEDGMENTS**

We thank Wendy Johnston for technical support, the WI genome technology core for sequencing, David Garcia and Vikram Agarwal for helpful comments on the manuscript, and Igor Ulitsky and Nick Burton for helpful discussions. This work was supported by a grant (GM067031) from the NIH. D.B. is an Investigator of the Howard Hughes Medical Institute.

## FIGURE LEGENDS

### Figure 1. Identification of *C. elegans* lincRNA genes

(A) Pipeline for *de novo* gene annotation and identification of lincRNAs. See main text and supplemental methods for details.

(B) Venn diagram showing the overlap between the results of *de novo* gene annotation and modENCODE gene annotation.

(C) Venn diagram showing the overlap of candidate lincRNA loci that passed the indicated filters.

(D) Venn diagram showing the overlap of candidate ancRNA loci that passed the indicated filters.

(E) The fraction of potential lincRNAs that had 3P-seq supported poly(A)-sites. Shown are the numbers of genes, with the number of splicing/3' UTR isoforms in parenthesis.

(F) Diagram of trans-splicing by splice leader 1 (SL1). A chimeric read spanning the SL1-exon junction is diagnostic of trans-splicing.

(G) Number of chimeric reads and unique junctions mapping to the upstream regions of lincRNA and protein-coding genes. For protein-coding genes, 100 cohorts, each selected to match the set of lincRNA genes with respect to gene number and expression levels, were used to estimate the 90% confidence interval (error bar).

### Figure 2. Endo-siRNAs mapping antisense to lincRNAs

(A) Abundance of endo-siRNAs mapping antisense to 112 lincRNAs with mean RPKM  $\geq 1$ . The key indicates the log-scaled RPKM values (endo-siRNA reads per kilobase per million genomic mapping reads). The lincRNAs were sorted by the mean RPKM values (averaging RPKMs calculated from all 35 RNA-seq samples). The data used to make this heatmap are presented in Table S6.

(B) Improved annotations of loci corresponding to the top 30 22G-RNA clusters from the adult stage. The left panel shows the fractions of 22G-RNAs mapping to the antisense strand (red), sense strand (green), and intergenic or intronic region (gray) of protein-coding genes annotated in ce6. The right panel shows

the fractions of 22G-RNAs mapping to the indicated transcripts of the *de novo* gene annotation, highlighting those mapping antisense to new transcripts (orange). Clusters mapping antisense to either lincRNAs or newly annotated transcripts that satisfied only two of the three lincRNA filtering criteria are indicated (blue and gray asterisks, respectively) as are those mapping to antisense to pseudogenes (*T09F5.12*, *Y39E4B.14*, and *C47G2.6*).

(C) Improved annotations of loci corresponding to the top 30 26G-RNA clusters from the embryo stage. Otherwise, as in (B).

### Figure 3. lincRNA sequence composition and conservation

(A) A/U content of lincRNAs and ancRNAs, compared to that of mRNA 5' UTRs, 3' UTRs, and coding regions, and that of intergenic regions. Box and whisker plots indicate the median, interquartile range (IQR) between 25<sup>th</sup> and 75<sup>th</sup> percentiles (box), and 1.5 IQR (whisker).

(B) A/U content of lincRNAs antisense to abundant 22G-RNAs ( $\geq 5$  RPKM) and those antisense to less abundant or no 22G-RNAs ( $< 5$  RPKM). Otherwise, as in (A).

(C) The fraction of mRNAs containing annotated repeat elements.

(D) The fraction of lincRNAs containing annotated repeat elements.

(E) Fraction of residues aligned in multiple-genome alignments for the indicated mRNA and lincRNA regions. Control exons were generated by random selection of a length-matched region from intergenic space of the same chromosome; within this control region exons were assigned to the same relative positions as in the authentic lincRNA locus.

(F) Conservation of lincRNA and mRNA introns and exons. Shown are cumulative distributions of mean phastCons scores derived from the six-way whole-genome alignments (Siepel et al. 2005). Control exons were as in (E).



(G) Relationship between mapping to 22G-RNAs and sequence conservation. lincRNAs were assigned to three groups based on the abundance (RPKM) of antisense-mapping 22G-RNAs. Shown are cumulative distributions of mean phastCons scores (Siepel et al. 2005) for each group.

(H) Lengths of conserved regions within exons. For each exon that had an average phastCons score  $> 0$ , the maximum length of regions exceeding a phastCons score of 0.5 was measured. For CDS exons, 1000 length-matched exons were randomly selected from coding regions.

#### **Figure 4. Developmental- and stage-specific expression of lincRNAs**

(A) Differential expression of lincRNAs. For each lincRNA and mRNA, the maximum RPKM value from 10 distinct developmental stages (Table S1B) is plotted relative to the mean value for the remaining 9 stages. If the mean value was 0, a small value (0.1) was added to avoid the log 0 value error. For stages with multiple samples, the median value of RPKMs was used. The inset shows cumulative distributions of  $\log_2$ -scaled ratios of maximum and mean RPKMs for lincRNA and mRNAs.

(B) Dauer-specific expression of linc-3. Plotted are the RPKM values of linc-3 in 10 distinct stages.

(C) Four large lincRNA expression clusters over 35 different developmental stages/conditions (top key). Colored asterisks indicate lincRNA genes within 10 kb of each other. Within each cluster, lincRNAs are sorted based on their expression level (mean RPKM), with the expression level indicated at the far right. The five columns on the right show the abundance (RPKM) of endo-siRNAs mapping antisense to each lincRNA (bottom key).

(D) Correlation between lincRNA expression and that of their closest protein-coding gene. Shown is the average correlation for pairs with the indicated relative orientations (tandem, convergent, and divergent), considering only pairs within 1 kb of each other. As a control, mean correlations were also calculated for number-matched cohorts of random pairs of lincRNA and protein-coding genes. For comparison, mean correlations were calculated for number-matched cohorts of protein-coding gene

pairs. For both the controls and comparisons, the average correlation of 1000 cohorts is reported for each orientation, with error bars showing the 95% confident interval.

**Figure 5. Long-range expression correlations involving the dauer-specific *linc-3*.**

(A) Expression of genes located within a 200 kb region centered on *linc-3*. The RNA-seq tracks illustrate that *linc-3* and many other genes in the region were expressed higher in dauer entry and dauer stages compared with dauer exit and L3 stages. The inset illustrates the gene structure of *linc-3* and its very high expression during dauer entry, with a read maximum exceeding that of any other gene in the region. The gene models are color coded based on the correlation between their expression and that of *linc-3* (key).

(B) The expression profile of *linc-3* across 35 different developmental stages/conditions.

(C) The expression profile of the 59 genes within 100 kb of the *linc-3* gene, visualized by plotting the mean z scores for each stage/condition. The error bars indicate standard deviation.

**Figure 6. A short conserved segment of *linc-85* complementary to members of the Major Sperm**

**Protein family.** Conservation and alignment tracks show a ~70 nt segment conserved in four additional sequenced species. This segment has extensive complementarity to 37 members of the Major Sperm Protein (MSP) family (E-value <  $10^{-5}$ ), including some hypothetical genes (e.g., *ZK1248.17*).

**Table 1.** lincRNAs antisense to endo-siRNAs (small-RNA RPKM  $\geq 5$ ) in L4 and adult stages. When analyzing individual stages, the RNA-seq RPKM was determined for that stage. When analyzing multiple stages, mean RPKM was used. Differences in the fraction matching endo-siRNAs between lincRNAs and mRNAs (both RPKM  $\geq 1$ ) were tested for significance using the Fisher's exact test.

	RNA-seq RPKM $\geq 1$		RNA-seq RPKM $< 1$		RNA-seq RPKM $\geq 1$	RNA-seq RPKM $< 1$	Difference between lincRNA & mRNA ( <i>P</i> value)
	lincRNAs	lincRNAs antisense to endo-siRNAs	lincRNAs	lincRNAs antisense to endo-siRNAs	mRNA antisense to endo-siRNAs		
22G-RNAs in L4	74	21 (28.4%)	177	14 (7.9%)	7.8%	6.0%	$3 \times 10^{-8}$
22G-RNAs in adults	68	20 (29.4%)	183	8 (4.4%)	7.9%	3.2%	$2 \times 10^{-7}$
22G-RNAs in adult WAGO1 IP	68	16 (23.5%)	183	19 (10.4%)	10.6%	7.4%	0.0018
22G-RNAs in adult CSR1 IP	68	22 (32.4%)	183	11 (6.0%)	35.1%	4.0%	0.73
22G-RNAs in both stages & IPs	112	37 (33.0%)	139	16 (11.5%)	35.7%	9.2%	0.75
26G-RNAs in embryo	76	16 (21.0%)	175	8 (4.5%)	0.25%	0.25%	$10^{-25}$
26G-RNAs in L4	74	21 (28.4%)	177	4 (2.3%)	4.3%	0.34%	$10^{-12}$
26G-RNAs in both stages	112	28 (25.0%)	139	8 (5.8%)	3.8%	0.71%	$10^{-14}$

## REFERENCES

- Ambros, V., R. C. Lee, A. Lavanway, P. T. Williams and D. Jewell 2003. MicroRNAs and other tiny endogenous RNAs in *C. elegans*. *Curr Biol* 13(10): 807-18.
- Batista, P. J., J. G. Ruby, J. M. Claycomb, R. Chiang, N. Fahlgrén, K. D. Kasschau, D. A. Chaves, W. Gu, J. J. Vasale, S. Duan, et al. 2008. PRG-1 and 21U-RNAs interact to form the piRNA complex required for fertility in *C. elegans*. *Mol Cell* 31(1): 67-78.
- Birney, E., J. A. Stamatoyannopoulos, A. Dutta, R. Guigo, T. R. Gingeras, E. H. Margulies, Z. Weng, M. Snyder, E. T. Dermitzakis, R. E. Thurman, et al. 2007. Identification and analysis of functional elements in 1% of the human genome by the ENCODE pilot project. *Nature* 447(7146): 799-816.
- Blumenthal, T. and K. S. Gleason 2003. *Caenorhabditis elegans* operons: form and function. *Nat Rev Genet* 4(2): 112-20.
- Blumenthal, T. and K. Steward 1997. RNA Processing and Gene Structure.
- Borsani, G., R. Tonlorenzi, M. C. Simmler, L. Dandolo, D. Arnaud, V. Capra, M. Grompe, A. Pizzuti, D. Muzny, C. Lawrence, et al. 1991. Characterization of a murine gene expressed from the inactive X chromosome. *Nature* 351(6324): 325-9.
- Brockdorff, N., A. Ashworth, G. F. Kay, V. M. McCabe, D. P. Norris, P. J. Cooper, S. Swift and S. Rastan 1992. The product of the mouse Xist gene is a 15 kb inactive X-specific transcript containing no conserved ORF and located in the nucleus. *Cell* 71(3): 515-26.
- Brown, C. J., B. D. Hendrich, J. L. Rupert, R. G. Lafreniere, Y. Xing, J. Lawrence and H. F. Willard 1992. The human XIST gene: analysis of a 17 kb inactive X-specific RNA that contains conserved repeats and is highly localized within the nucleus. *Cell* 71(3): 527-42.
- Burkhart, K. B., S. Guang, B. A. Buckley, L. Wong, A. F. Bochner and S. Kennedy 2011. A pre-mRNA-associating factor links endogenous siRNAs to chromatin regulation. *PLoS Genet* 7(8): e1002249.
- Cabili, M. N., C. Trapnell, L. Goff, M. Koziol, B. Tazon-Vega, A. Regev and J. L. Rinn 2011. Integrative annotation of human large intergenic noncoding RNAs reveals global properties and specific subclasses. *Genes Dev* 25(18): 1915-27.
- Carninci, P., T. Kasukawa, S. Katayama, J. Gough, M. C. Frith, N. Maeda, R. Oyama, T. Ravasi, B. Lenhard, C. Wells, et al. 2005. The transcriptional landscape of the mammalian genome. *Science* 309(5740): 1559-63.
- Chen, N. and L. D. Stein 2006. Conservation and functional significance of gene topology in the genome of *Caenorhabditis elegans*. *Genome Res* 16(5): 606-17.
- Chen, W. H., J. de Meaux and M. J. Lercher 2010. Co-expression of neighbouring genes in Arabidopsis: separating chromatin effects from direct interactions. *BMC Genomics* 11: 178.
- Clark, M. B., P. P. Amaral, F. J. Schlesinger, M. E. Dinger, R. J. Taft, J. L. Rinn, C. P. Ponting, P. F. Stadler, K. V. Morris, A. Morillon, et al. 2011. The reality of pervasive transcription. *PLoS Biol* 9(7): e1000625.
- Claycomb, J. M., P. J. Batista, K. M. Pang, W. Gu, J. J. Vasale, J. C. van Wolfswinkel, D. A. Chaves, M. Shirayama, S. Mitani, R. F. Ketting, et al. 2009. The Argonaute CSR-1 and its 22G-RNA cofactors are required for holocentric chromosome segregation. *Cell* 139(1): 123-34.
- Edgar, R., M. Domrachev and A. E. Lash 2002. Gene Expression Omnibus: NCBI gene expression and hybridization array data repository. *Nucleic Acids Res* 30(1): 207-10.
- Fischer, S. E., T. A. Montgomery, C. Zhang, N. Fahlgrén, P. C. Breen, A. Hwang, C. M. Sullivan, J. C. Carrington and G. Ruvkun 2011. The ERI-6/7 helicase acts at the first stage of an siRNA amplification pathway that targets recent gene duplications. *PLoS Genet* 7(11): e1002369.
- Gerstein, M. B., Z. J. Lu, E. L. Van Nostrand, C. Cheng, B. I. Arshinoff, T. Liu, K. Y. Yip, R. Robilotto, A. Rechtsteiner, K. Ikegami, et al. 2010. Integrative analysis of the *Caenorhabditis elegans* genome by the modENCODE project. *Science* 330(6012): 1775-87.

- Goodrich, J. A. and J. F. Kugel 2006. Non-coding-RNA regulators of RNA polymerase II transcription. *Nat Rev Mol Cell Biol* 7(8): 612-6.
- Grabherr, M. G., B. J. Haas, M. Yassour, J. Z. Levin, D. A. Thompson, I. Amit, X. Adiconis, L. Fan, R. Raychowdhury, Q. Zeng, et al. 2011. Full-length transcriptome assembly from RNA-Seq data without a reference genome. *Nat Biotechnol* 29(7): 644-52.
- Gu, S. G., J. Pak, S. Guang, J. M. Maniar, S. Kennedy and A. Fire 2012. Amplification of siRNA in *Caenorhabditis elegans* generates a transgenerational sequence-targeted histone H3 lysine 9 methylation footprint. *Nat Genet*.
- Gu, W., M. Shirayama, D. Conte, Jr., J. Vasale, P. J. Batista, J. M. Claycomb, J. J. Moresco, E. M. Youngman, J. Keys, M. J. Stoltz, et al. 2009. Distinct argonaute-mediated 22G-RNA pathways direct genome surveillance in the *C. elegans* germline. *Mol Cell* 36(2): 231-44.
- Guang, S., A. F. Bochner, K. B. Burkhardt, N. Burton, D. M. Pavelec and S. Kennedy 2010. Small regulatory RNAs inhibit RNA polymerase II during the elongation phase of transcription. *Nature* 465(7301): 1097-101.
- Gupta, R. A., N. Shah, K. C. Wang, J. Kim, H. M. Horlings, D. J. Wong, M. C. Tsai, T. Hung, P. Argani, J. L. Rinn, et al. 2010. Long non-coding RNA HOTAIR reprograms chromatin state to promote cancer metastasis. *Nature* 464(7291): 1071-6.
- Guttman, M., I. Amit, M. Garber, C. French, M. F. Lin, D. Feldser, M. Huarte, O. Zuk, B. W. Carey, J. P. Cassady, et al. 2009. Chromatin signature reveals over a thousand highly conserved large non-coding RNAs in mammals. *Nature* 458(7235): 223-7.
- Guttman, M., M. Garber, J. Z. Levin, J. Donaghey, J. Robinson, X. Adiconis, L. Fan, M. J. Koziol, A. Gnirke, C. Nusbaum, et al. 2010. Ab initio reconstruction of cell type-specific transcriptomes in mouse reveals the conserved multi-exonic structure of lincRNAs. *Nat Biotechnol* 28(5): 503-10.
- Hillier, L. W., V. Reinke, P. Green, M. Hirst, M. A. Marra and R. H. Waterston 2009. Massively parallel sequencing of the polyadenylated transcriptome of *C. elegans*. *Genome Res* 19(4): 657-66.
- Huarte, M., M. Guttman, D. Feldser, M. Garber, M. J. Koziol, D. Kenzelmann-Broz, A. M. Khalil, O. Zuk, I. Amit, M. Rabani, et al. 2010. A large intergenic noncoding RNA induced by p53 mediates global gene repression in the p53 response. *Cell* 142(3): 409-19.
- Huarte, M. and J. L. Rinn 2010. Large non-coding RNAs: missing links in cancer? *Hum Mol Genet* 19(R2): R152-61.
- Ingolia, N. T., L. F. Lareau and J. S. Weissman 2011. Ribosome profiling of mouse embryonic stem cells reveals the complexity and dynamics of mammalian proteomes. *Cell* 147(4): 789-802.
- Jan, C. H., R. C. Friedman, J. G. Ruby and D. P. Bartel 2011. Formation, regulation and evolution of *Caenorhabditis elegans* 3'UTRs. *Nature* 469(7328): 97-101.
- Ji, P., S. Diederichs, W. Wang, S. Boing, R. Metzger, P. M. Schneider, N. Tidow, B. Brandt, H. Buerger, E. Bulk, et al. 2003. MALAT-1, a novel noncoding RNA, and thymosin beta4 predict metastasis and survival in early-stage non-small cell lung cancer. *Oncogene* 22(39): 8031-41.
- Jia, H., M. Osak, G. K. Bogu, L. W. Stanton, R. Johnson and L. Lipovich 2010. Genome-wide computational identification and manual annotation of human long noncoding RNA genes. *RNA* 16(8): 1478-87.
- Jurka, J. 2000. Repbase update: a database and an electronic journal of repetitive elements. *Trends Genet* 16(9): 418-20.
- Kensche, P. R., M. Oti, B. E. Dutilh and M. A. Huynen 2008. Conservation of divergent transcription in fungi. *Trends Genet* 24(5): 207-11.
- Kim, K., K. Sato, M. Shibuya, D. M. Zeiger, R. A. Butcher, J. R. Ragains, J. Clardy, K. Touhara and P. Sengupta 2009. Two chemoreceptors mediate developmental effects of dauer pheromone in *C. elegans*. *Science* 326(5955): 994-8.

- Kim, T. K., M. Hemberg, J. M. Gray, A. M. Costa, D. M. Bear, J. Wu, D. A. Harmin, M. Laptewicz, K. Barbara-Haley, S. Kuersten, et al. 2010. Widespread transcription at neuronal activity-regulated enhancers. *Nature* 465(7295): 182-7.
- Korbel, J. O., L. J. Jensen, C. von Mering and P. Bork 2004. Analysis of genomic context: prediction of functional associations from conserved bidirectionally transcribed gene pairs. *Nat Biotechnol* 22(7): 911-7.
- Koziol, M. J. and J. L. Rinn 2011. RNA traffic control of chromatin complexes. *Curr Opin Genet Dev* 20(2): 142-8.
- Lagos-Quintana, M., R. Rauhut, A. Yalcin, J. Meyer, W. Lendeckel and T. Tuschl 2002. Identification of tissue-specific microRNAs from mouse. *Curr Biol* 12(9): 735-9.
- Lall, S., C. C. Friedman, M. Jankowska-Anyszka, J. Stepinski, E. Darzynkiewicz and R. E. Davis 2004. Contribution of trans-splicing, 5' -leader length, cap-poly(A) synergism, and initiation factors to nematode translation in an *Ascaris suum* embryo cell-free system. *J Biol Chem* 279(44): 45573-85.
- Lamm, A. T., M. R. Stadler, H. Zhang, J. I. Gent and A. Z. Fire 2011. Multimodal RNA-seq using single-strand, double-strand, and CirLigase-based capture yields a refined and extended description of the *C. elegans* transcriptome. *Genome Res* 21(2): 265-75.
- Larschan, E., E. P. Bishop, P. V. Kharchenko, L. J. Core, J. T. Lis, P. J. Park and M. I. Kuroda 2011. X chromosome dosage compensation via enhanced transcriptional elongation in *Drosophila*. *Nature* 471(7336): 115-8.
- Lu, Z. J., K. Y. Yip, G. Wang, C. Shou, L. W. Hillier, E. Khurana, A. Agarwal, R. Auerbach, J. Rozowsky, C. Cheng, et al. 2010. Prediction and characterization of noncoding RNAs in *C. elegans* by integrating conservation, secondary structure, and high-throughput sequencing and array data. *Genome Res* 21(2): 276-85.
- Mangone, M., A. P. Manoharan, D. Thierry-Mieg, J. Thierry-Mieg, T. Han, S. D. Mackowiak, E. Mis, C. Zegar, M. R. Gutwein, V. Khivansara, et al. 2010. The landscape of *C. elegans* 3'UTRs. *Science* 329(5990): 432-5.
- Martianov, I., A. Ramadass, A. Serra Barros, N. Chow and A. Akoulitchev 2007. Repression of the human dihydrofolate reductase gene by a non-coding interfering transcript. *Nature* 445(7128): 666-70.
- McGrath, P. T., Y. Xu, M. Ailion, J. L. Garrison, R. A. Butcher and C. I. Bargmann 2011. Parallel evolution of domesticated *Caenorhabditis* species targets pheromone receptor genes. *Nature* 477(7364): 321-5.
- Mercer, T. R., M. E. Dinger and J. S. Mattick 2009. Long non-coding RNAs: insights into functions. *Nat Rev Genet* 10(3): 155-9.
- Montgomery, M. K., S. Xu and A. Fire 1998. RNA as a target of double-stranded RNA-mediated genetic interference in *Caenorhabditis elegans*. *Proc Natl Acad Sci U S A* 95(26): 15502-7.
- Numata, K., A. Kanai, R. Saito, S. Kondo, J. Adachi, L. G. Wilming, D. A. Hume, Y. Hayashizaki and M. Tomita 2003. Identification of putative noncoding RNAs among the RIKEN mouse full-length cDNA collection. *Genome Res* 13(6B): 1301-6.
- Okazaki, Y., M. Furuno, T. Kasukawa, J. Adachi, H. Bono, S. Kondo, I. Nikaido, N. Osato, R. Saito, H. Suzuki, et al. 2002. Analysis of the mouse transcriptome based on functional annotation of 60,770 full-length cDNAs. *Nature* 420(6915): 563-73.
- Orom, U. A., T. Derrien, M. Beringer, K. Gumireddy, A. Gardini, G. Bussotti, F. Lai, M. Zytnicki, C. Notredame, Q. Huang, et al. 2010. Long noncoding RNAs with enhancer-like function in human cells. *Cell* 143(1): 46-58.
- Pak, J. and A. Fire 2007. Distinct populations of primary and secondary effectors during RNAi in *C. elegans*. *Science* 315(5809): 241-4.

- Pauli, A., J. L. Rinn and A. F. Schier 2011a. Non-coding RNAs as regulators of embryogenesis. *Nat Rev Genet* 12(2): 136-49.
- Pauli, A., E. Valen, M. F. Lin, M. Garber, N. L. Vastenhouw, J. Z. Levin, L. Fan, A. Sandelin, J. L. Rinn, A. Regev, et al. 2011b. Systematic identification of long noncoding RNAs expressed during zebrafish embryogenesis. *Genome Res*.
- Rinn, J. L., M. Kertesz, J. K. Wang, S. L. Squazzo, X. Xu, S. A. Bruggmann, L. H. Goodnough, J. A. Helms, P. J. Farnham, E. Segal, et al. 2007. Functional demarcation of active and silent chromatin domains in human HOX loci by noncoding RNAs. *Cell* 129(7): 1311-23.
- Ruby, J. G., C. Jan, C. Player, M. J. Axtell, W. Lee, C. Nusbaum, H. Ge and D. P. Bartel 2006. Large-scale sequencing reveals 21U-RNAs and additional microRNAs and endogenous siRNAs in *C. elegans*. *Cell* 127(6): 1193-207.
- Sharan, R., A. Maron-Katz and R. Shamir 2003. CLICK and EXPANDER: a system for clustering and visualizing gene expression data. *Bioinformatics* 19(14): 1787-99.
- Siepel, A., G. Bejerano, J. S. Pedersen, A. S. Hinrichs, M. Hou, K. Rosenbloom, H. Clawson, J. Spieth, L. W. Hillier, S. Richards, et al. 2005. Evolutionarily conserved elements in vertebrate, insect, worm, and yeast genomes. *Genome Res* 15(8): 1034-50.
- Spieth, J., G. Brooke, S. Kuersten, K. Lea and T. Blumenthal 1993. Operons in *C. elegans*: polycistronic mRNA precursors are processed by trans-splicing of SL2 to downstream coding regions. *Cell* 73(3): 521-32.
- Trapnell, C., L. Pachter and S. L. Salzberg 2009. TopHat: discovering splice junctions with RNA-Seq. *Bioinformatics* 25(9): 1105-11.
- Trapnell, C., B. A. Williams, G. Pertea, A. Mortazavi, G. Kwan, M. J. van Baren, S. L. Salzberg, B. J. Wold and L. Pachter 2010. Transcript assembly and quantification by RNA-Seq reveals unannotated transcripts and isoform switching during cell differentiation. *Nat Biotechnol* 28(5): 511-5.
- Tripathi, V., J. D. Ellis, Z. Shen, D. Y. Song, Q. Pan, A. T. Watt, S. M. Freier, C. F. Bennett, A. Sharma, P. A. Bubulya, et al. 2010. The nuclear-retained noncoding RNA MALAT1 regulates alternative splicing by modulating SR splicing factor phosphorylation. *Mol Cell* 39(6): 925-38.
- Tsai, M. C., O. Manor, Y. Wan, N. Mosammamaparast, J. K. Wang, F. Lan, Y. Shi, E. Segal and H. Y. Chang 2010. Long noncoding RNA as modular scaffold of histone modification complexes. *Science* 329(5992): 689-93.
- Tsai, M. C., R. C. Spitale and H. Y. Chang 2011. Long intergenic noncoding RNAs: new links in cancer progression. *Cancer Res* 71(1): 3-7.
- Ulitsky, I., A. Shkumatava, C. H. Jan, H. Sive and D. P. Bartel 2011. Conserved Function of lincRNAs in Vertebrate Embryonic Development despite Rapid Sequence Evolution. *Cell* 147(7): 1537-50.
- Wang, G. Z., M. J. Lercher and L. D. Hurst 2011a. Transcriptional coupling of neighboring genes and gene expression noise: evidence that gene orientation and noncoding transcripts are modulators of noise. *Genome Biol Evol* 3: 320-31.
- Wang, X., S. Arai, X. Song, D. Reichart, K. Du, G. Pascual, P. Tempst, M. G. Rosenfeld, C. K. Glass and R. Kurokawa 2008. Induced ncRNAs allosterically modify RNA-binding proteins in cis to inhibit transcription. *Nature* 454(7200): 126-30.
- Wang, Y., J. Chen, G. Wei, H. He, X. Zhu, T. Xiao, J. Yuan, B. Dong, S. He, G. Skogerbo, et al. 2011b. The *Caenorhabditis elegans* intermediate-size transcriptome shows high degree of stage-specific expression. *Nucleic Acids Res*.
- Washietl, S., S. Findeiss, S. A. Muller, S. Kalkhof, M. von Bergen, I. L. Hofacker, P. F. Stadler and N. Goldman 2011. RNAcode: robust discrimination of coding and noncoding regions in comparative sequence data. *RNA* 17(4): 578-94.
- Zhao, J., B. K. Sun, J. A. Erwin, J. J. Song and J. T. Lee 2008. Polycomb proteins targeted by a short repeat RNA to the mouse X chromosome. *Science* 322(5902): 750-6.

Figure 1.

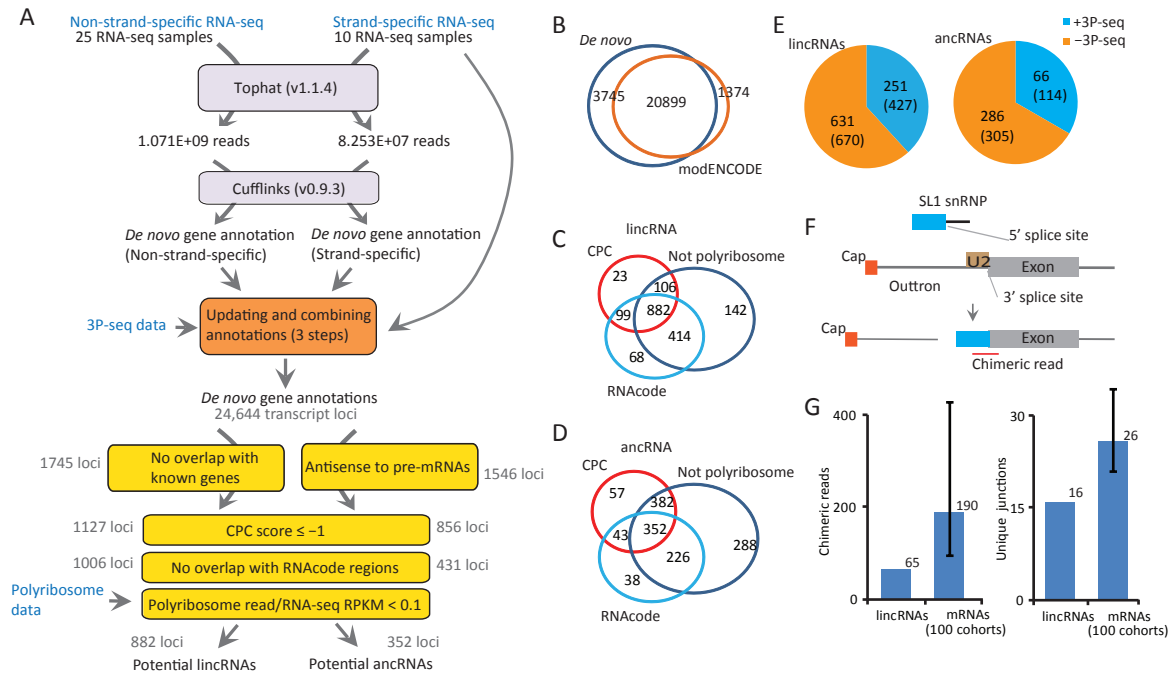




Figure 2.

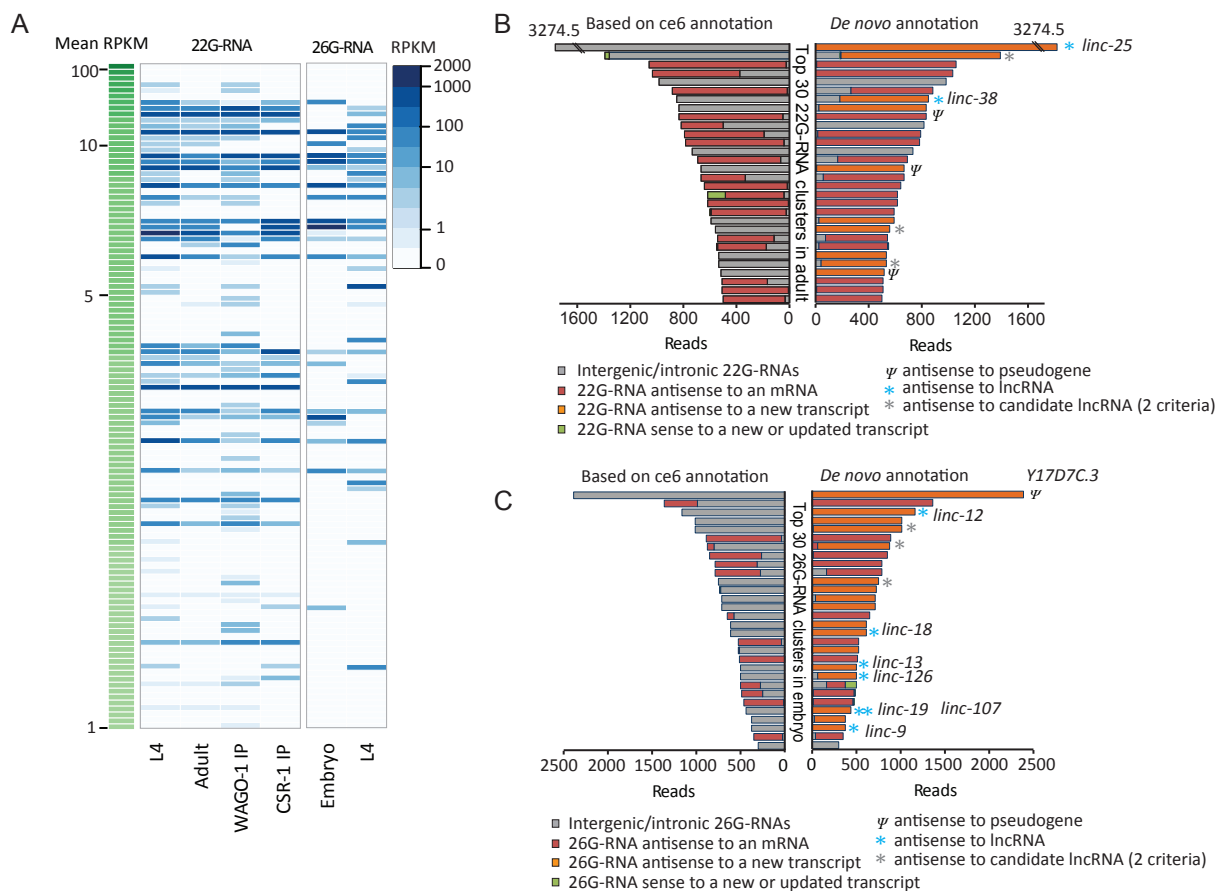


Figure 3.

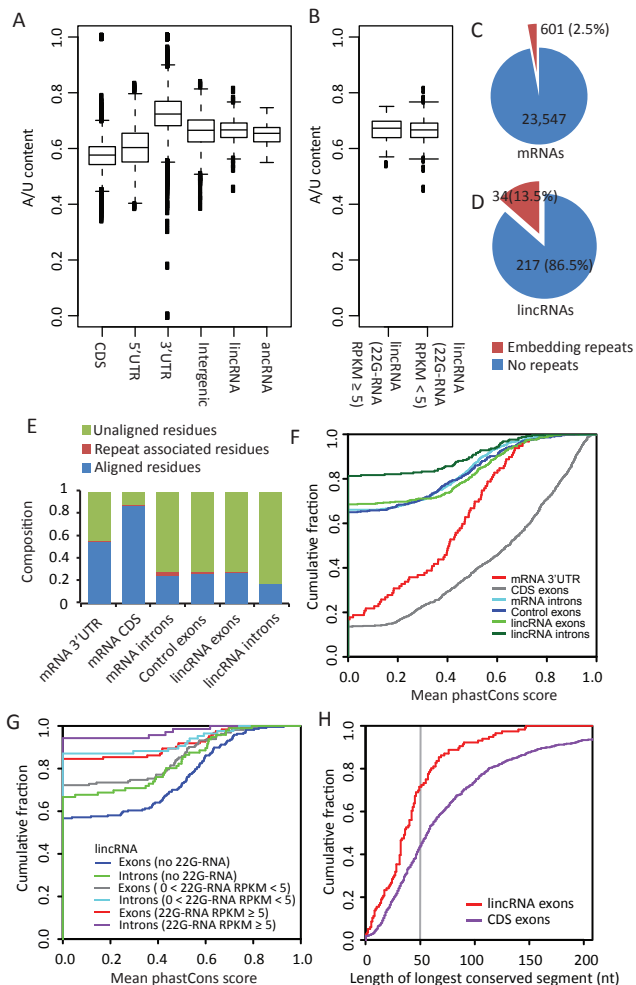




Figure 5.

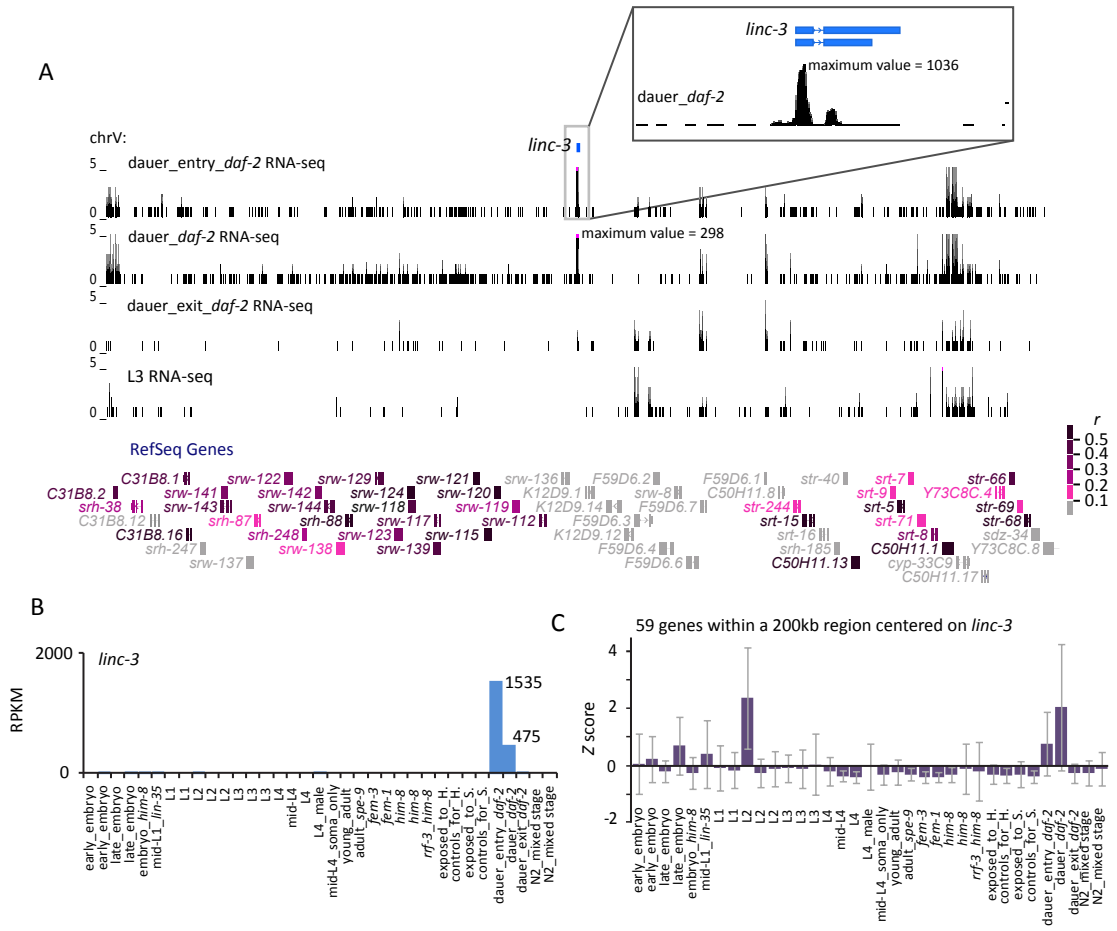


Figure 6.

